

# Diffractive and Exclusive Processes in Electron-Proton Scattering at the LHeC

Paul Newman<sup>1</sup>

*School of Physics, University of Birmingham, B15 2TT, UK*

**Abstract.** The sensitivity of diffractive processes at the LHeC to the onset of parton saturation phenomena at low Bjorken- $x$  is discussed in the context of simulated measurements of exclusive  $J/\psi$  photoproduction, Deeply Virtual Compton Scattering and Inclusive Diffractive Deep Inelastic Scattering.

**Keywords:** Diffraction, Low  $x$ , Saturation, LHeC

**PACS:** 12.38.-t, 24.85.+p

## INTRODUCTION

Probably the biggest open question in low Bjorken- $x$  physics is the mechanism by which the growth of cross sections and parton densities with decreasing  $x$  [1] is tamed, such that unitarity constraints are satisfied. Despite detailed investigation, such ‘saturation’ effects have not been firmly established in HERA data, though hints at small photon virtualities,  $Q^2 \lesssim 1 \text{ GeV}^2$ , have aided the development of models of the non-linear dynamics which are believed to be responsible [2, 3]. The proposed Large Hadron electron Collider (LHeC) [4, 5, 6] would address the saturation problem by providing electron-hadron collisions at unprecedented centre-of-mass energies, accessing the low  $x$  regime in which unitarisation effects are expected, at sufficiently large  $Q^2$  values for quarks and gluons to be good degrees of freedom and for the rise of the gluon density with decreasing  $x$  to be substantial. This contribution [7] discusses the role which diffractive channels can be expected to play in this exploration, alongside inclusive electron-proton scattering cross sections at low  $x$  [8] and similar studies of electron scattering from heavy ions [9].

The generic benefits of diffractive channels in searching for saturation effects are two-fold. Firstly, the lowest order interpretation of diffraction in terms of two-gluon exchange [10] gives quadratic sensitivity to saturation effects, in contrast to the linear dependences of inclusive processes. Secondly, through the measurement of the squared four-momentum transfer,  $t$ , the impact parameter dependence can be assessed, with the expectation that unitarisation effects set in first for the large  $t$ , small impact parameter, region, corresponding to the central, densest packed, part of the hadron target.

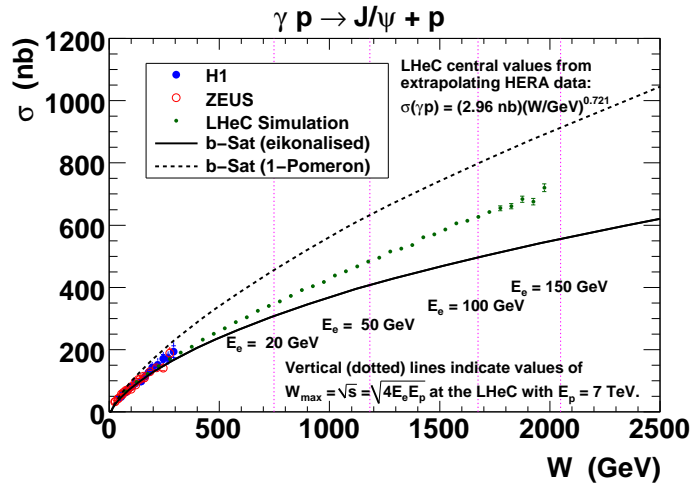
In the following sections, three selected case studies of simulated diffractive measurements at an LHeC are described. More details can be found in [5].

---

<sup>1</sup> On behalf of the LHeC Study Group.

## ELASTIC $J/\psi$ PHOTOPRODUCTION

The photoproduction (studied via electroproduction at  $Q^2 \rightarrow 0$ ) of  $J/\psi$  mesons,  $\gamma p \rightarrow J/\psi p$ , with subsequent decay of the  $J/\psi$  to leptons, is possibly the most promising diffractive channel in terms of sensitivity to saturation phenomena. From the theoretical perspective, its interpretation in terms of two-gluon exchange is relatively cleanly established [11] and, due to the approximately equal sharing of the  $J/\psi$  energy by the charm and anticharm quarks, the vector meson wavefunction is well known compared for example to that of a  $\rho^0$  meson. The experimental signature is very clean, with an entirely empty detector except for the two leptons and the cross section is large compared for example with  $\Upsilon$  production. Given that the process probes gluon momentum fractions  $x_g \sim (Q^2 + M_{J/\psi}^2)/(Q^2 + W^2)$  at an effective scale  $\overline{Q^2} \sim (Q^2 + M_{J/\psi}^2)/4$ , where  $W$  is the  $\gamma p$  centre of mass energy, the region in which saturation phenomena are expected to set in [2, 3] is well within the kinematic reach of the LHeC.



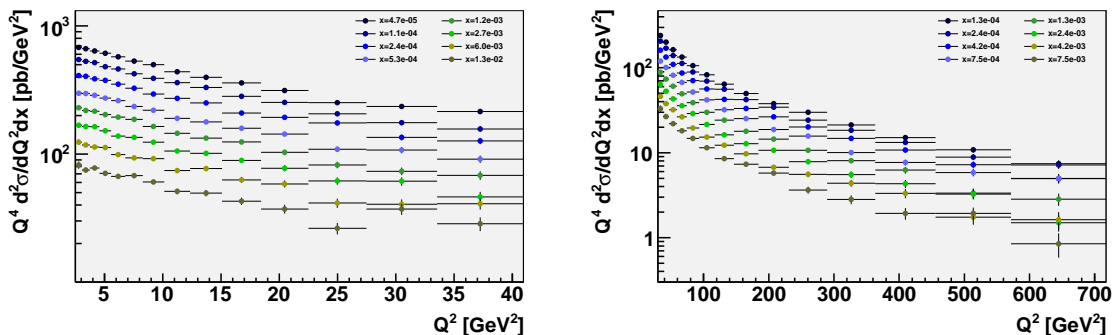
**FIGURE 1.** Simulated LHeC measurements of the photoproduction cross section  $\sigma(\gamma p \rightarrow J/\psi p)$ , together with previous data from HERA and dipole model predictions with and without saturation effects.

Figure 1 shows a simulated LHeC measurement of the  $W$  dependence of  $J/\psi$  photoproduction, integrated over  $t$ . The simulation assumes that muons can be detected and their momenta measured precisely to angles within  $1^\circ$  of the beampipe [12] and is based on an integrated luminosity of  $2 \text{ fb}^{-1}$ , comfortably obtainable within one year according to the current best estimates [13, 14]. Acceptances are evaluated using the DIFFVM Monte Carlo generator [15]. HERA data [16, 17] are shown in addition to the LHeC simulation. The upper kinematic limits in  $W$  are illustrated for electron beam energies of 20, 50, 100 and 150 GeV. The data are plotted with a cross section based on a power law extrapolation of HERA data. The predicted cross section from the  $b$ -Sat dipole model [3] is shown for both the (non-saturating) case of a single pomeron exchange and for an eikonalised sum of multiple pomeron exchanges, illustrating the influence of unitarisation effects according to this model. Even for relatively modest electron beam energies, it should easily be possible to distinguish the two cases and to study the onset of saturation effects as a function of both  $W$  and  $t$ , as explored further in [5].

## DEEPLY VIRTUAL COMPTON SCATTERING

Deeply virtual Compton scattering (DVCS,  $\gamma^* p \rightarrow \gamma p$ ) is even cleaner than  $J/\psi$  production from the theoretical point of view, with no wavefunction uncertainty. As well as giving sensitivity to saturation phenomena, the DVCS process is uniquely sensitive to the Generalised Parton Distributions (GPDs) of the proton [18]. However, the cross section is suppressed relative to vector meson production processes by an additional electromagnetic coupling and the HERA data [19, 20, 21] are correspondingly limited.

Simulations of the DVCS measurement possibilities with the LHeC have been made using the MILOU Monte Carlo generator [22], with the DVCS cross section taken from [23]. Detector acceptance cuts at either  $1^\circ$  or  $10^\circ$  are placed on the polar angle of the final state electron and photon. Based on experience with controlling backgrounds in HERA DVCS measurements [19, 20, 21], an additional cut is placed on the transverse momentum  $P_T^\gamma$  of the final state photon.



**FIGURE 2.** Simulated DVCS cross section measurements,  $\sigma(ep \rightarrow e\gamma p)$ , for an LHeC configuration which is optimised to (a) high detector acceptance and (b) high luminosity.

A simulation of a possible LHeC DVCS measurement is shown double differentially in  $x$  and  $Q^2$  in Fig. 2a for a very modest luminosity scenario ( $1 \text{ fb}^{-1}$ ) in which the electron beam energy is 50 GeV, the detector acceptance extends to  $1^\circ$  and photon measurements are possible down to  $P_T^\gamma = 2 \text{ GeV}$ . High precision is possible throughout the region  $2.5 < Q^2 < 40 \text{ GeV}^2$  for  $x$  values extending down to  $\sim 5 \times 10^{-5}$ .

If the detector acceptance extends to only  $10^\circ$ , the  $P_T^\gamma$  cut no longer plays such an important role. Although the low  $Q^2$  acceptance is lost in this scenario, a larger integrated luminosity is likely to be obtainable, which will allow precise measurements for  $Q^2 \gtrsim 50 \text{ GeV}^2$ , a region which has not been explored previously. In the simulation shown in Fig. 2b, a luminosity of  $100 \text{ fb}^{-1}$  is considered, resulting in precise measurements extending to  $Q^2 > 500 \text{ GeV}^2$ , well beyond the range explored for GPD-sensitive processes to date.

## INCLUSIVE DEEP INELASTIC DIFFRACTION

Approximately 10% of all low- $x$  DIS events are of the general diffractive type,  $ep \rightarrow eXp$  (figure 3a). In contrast to the vector meson production and DVCS processes the bulk of

these diffractive DIS (DDIS) events exhibit a very similar (leading twist)  $Q^2$  dependence to that of the fully inclusive DIS cross section. The most common interpretation is that a colour-singlet combination of partons (a ‘pomeron’) is exchanged, the structure of which is probed by the virtual photon. Due to the lack of colour flow, DDIS events are characterised by a large ‘rapidity gap’ in the distribution of final state hadrons, adjacent to the scattered proton, of size  $\Delta\eta \simeq \ln(1/x_{\text{P}})$ . DDIS can thus be identified by the experimental signatures of either a leading proton [24, 25] or the presence of a large rapidity gap [26, 24]. One of the main achievements at HERA has been the development of an understanding of DDIS in terms of parton dynamics and QCD, with the partonic structure of the exchanged pomeron now well understood [26, 27].

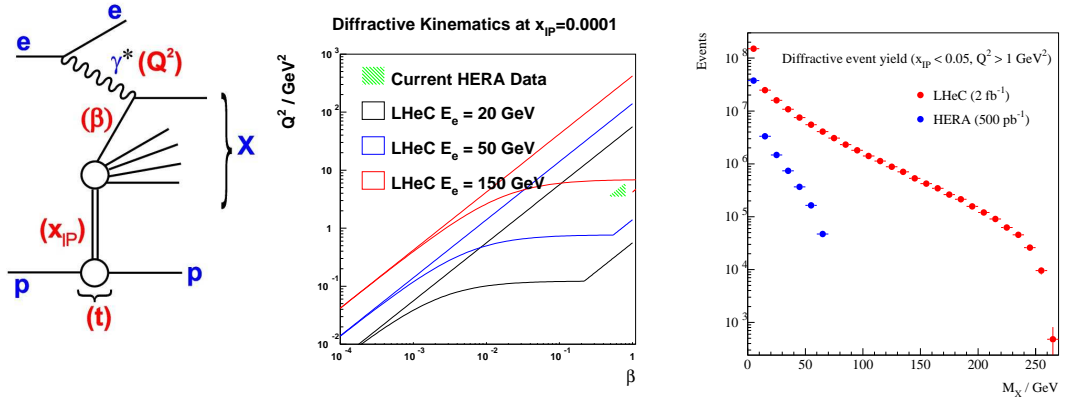


**FIGURE 3.** (a) Illustration of the kinematic variables used to describe inclusive diffractive DIS. (b) Accessible  $(\beta, Q^2)$  kinematic plane at fixed  $x_{\text{P}} = 0.0001$  for HERA and three different LHeC scenarios. (c) Simulated distribution in diffractive dissociation mass  $M_X$  for a modest estimate of the annual LHeC luminosity, compared with the full available sample from HERA.

The LHeC will offer the opportunity to study diffractive DIS in an unprecedented kinematic range. The diffractive kinematic plane is illustrated in Fig. 3b for an example pomeron momentum fraction of  $x_{\text{P}} = 0.0001$  for three different LHeC electron beam energies. This  $x_{\text{P}}$  value is representative of the possibilities using the large rapidity gap technique, whereas higher fractional momenta  $x_{\text{P}} \sim 0.01$  can be accessed with the proposed proton spectrometer [28].

It is clear that the LHeC will provide a much increased reach compared with HERA towards low values of  $x_{\text{P}}$ , where the interpretation of diffractive events is not complicated by the presence of sub-leading meson exchanges, rapidity gaps are large and diffractive event selection systematics are correspondingly small. The range in the fractional struck quark momentum  $\beta$  extends by a factor of around 20 below that accessible at HERA. Large improvements in diffractive parton density extractions are likely to be possible; in addition to the extended phase space in  $\beta$ , the extension towards larger  $Q^2$  increases the lever-arm for extracting the diffractive gluon density and opens the possibility of significant weak gauge boson exchange, which would allow a quark flavour decomposition for the first time.

The previously unexplored diffractive DIS region of very low  $\beta$  is of particular interest. Here, diffractively produced systems will be created with unprecedented invariant masses. Figure 3c shows a comparison between HERA and the LHeC in terms of the

$M_X$  distribution which could be produced in diffractive processes with  $x_p < 0.05$  (using the RAPGAP Monte Carlo model [29]) assuming one year of running at three LHeC electron beam energy choices. Diffractive masses up to several hundred GeV are accessible with reasonable rates, such that diffractive final states involving high transverse momentum jets, beauty quarks,  $W$  and  $Z$  bosons, or even exotic states with  $1^-$  quantum numbers, could be produced.

## ACKNOWLEDGMENTS

Thanks to the many colleagues who have worked on low  $x$  physics at the LHeC, in particular Nestor Armesto, Brian Cole, Laurent Favart, Anna Stasto and Graeme Watt.

## REFERENCES

1. H1 and ZEUS Collaborations, JHEP**01** (2010) 109.
2. K. Golec-Biernat and M. Wüsthoff, Phys. Rev. **D59** (1998) 014017; E. Iancu, K. Itakura and S. Munier, Phys. Lett. **B590** (2004), 199.
3. H. Kowalski, L. Motyka and G. Watt, Phys. Rev. D74 (2006) 074016.
4. J. Dainton et al., JINST **1**, P10001 (2006).
5. LHeC Study Group, *Conceptual Design Report for a Large Hadron Electron Collider at CERN*, in litt.
6. M. Klein, *Overview of the LHeC Project*, these proceedings.
7. Slides: <http://www.ep.ph.bham.ac.uk/exp/LHeC/talks/DIS11.Newman.pdf>.
8. A. Stasto, *Low  $x$  physics at the LHeC from Inclusive Measurements*, these proceedings.
9. B. Cole,  *$eA$  Physics with the LHeC*, these proceedings.
10. F. Low, Phys. Rev. **D12** (1975) 163; S. Nussinov, Phys. Rev. Lett. **34** (1975) 1286.
11. A. Martin et al., Phys. Lett. **B662** (2008) 252.
12. P. Kostka, *A Detector for the LHeC*, these proceedings.
13. A. Bogacz, *LHeC Linac-Ring Design*, these proceedings.
14. M. Fitterer, *LHeC Ring-Ring Design*, these proceedings.
15. B. List and A. Mastroberardino, *DIFFVM: A Monte Carlo generator for diffractive processes in  $ep$  scattering*, Proceedings of the Workshop on Monte Carlo Generators for HERA Physics (1999), DESY-PROC-1992-02 (1999) 396
16. ZEUS Collaboration, Eur. Phys. J. **C24** (2002) 345.
17. H1 Collaboration, Eur. Phys. J. **C46** (2006) 585.
18. M. Diehl, Phys. Rept. **388** (2003) 41.
19. H1 Collaboration, Phys. Lett. **B659** (2008) 796.
20. ZEUS Collaboration, JHEP **05** (2009) 108.
21. H1 Collaboration, Phys. Lett. **B681** (2009) 391.
22. E. Perez, L. Schoeffel and L. Favart, *MILOU: A Monte-Carlo for deeply virtual Compton scattering*, hep-ph/0411389
23. L. Frankfurt, A. Freund and M. Strikman, Phys. Rev. **D58** (1998) 114001.
24. ZEUS Collaboration, Nucl. Phys. **B816** (2009) 1.
25. H1 Collaboration, Eur. Phys. J. **C71** (2011) 1578.
26. H1 Collaboration, Eur. Phys. J. **C48** (2006) 715.
27. ZEUS Collaboration, Nucl. Phys. **B831** (2010) 1.
28. FP420 Collaboration, *Higgs and New Physics with Forward Protons at the LHC*, arXiv:0806.0302 [hep-ex].
29. H. Jung, Comp. Phys. Commun. **86** (1995) 147.